

Hurst entropy: A method to determine predictability in a binary series based on a fractal-related process

Mariana Sacrini Ayres Ferraz and Alexandre Hiroaki Kihara*

Centro de Matemática, Computação e Cognição (CMCC), Universidade Federal do ABC (UFABC), São Bernardo do Campo, São Paulo 09606-045, Brasil



(Received 29 October 2018; revised manuscript received 8 April 2019; published 14 June 2019)

Shannon's concept of information is related to predictability. In a binary series, the value of information relies on the frequency of 0's and 1's, or how it is expected to occur. However, information entropy does not consider the bias in randomness related to autocorrelation. In fact, it is possible for a binary temporal series to carry both short- and long-term memories related to the sequential distribution of 0's and 1's. Although the Hurst exponent measures the range of autocorrelation, there is a lack of mathematical connection between information entropy and autocorrelation present in the series. To fill this important gap, we combined numerical simulations and an analytical approach to determine how information entropy changes according to the frequency of 0's and 1's and the Hurst exponent. Indeed, we were able to determine how predictability depends on both parameters. Our findings are certainly useful to several fields when binary times series are applied, such as neuroscience to econophysics.

DOI: [10.1103/PhysRevE.99.062115](https://doi.org/10.1103/PhysRevE.99.062115)

I. INTRODUCTION

Predictability is usually defined as consistent repetition of a state, behavior, course of action, or the like, making it possible to know in advance what to expect. To this end, it might require the orderly observation of events, what in mathematical terms is referred to as a temporal series. In fact, several processes can be translated into temporal series, which are often binary. From such items, it is possible to cite neuronal spikes [1], spin dynamics [2], diffusion processes [3], cellular channel openings [4], experiences of success and failure [5], happiness and sadness, and fluctuations in the stock market [6]. Binary temporal series may show patterns made by sequences with distinct lengths of two symbols, such as 0's and 1's, which repeat over time. The appearance of such patterns allows one to distinguish between intrinsic behaviors of the data, such as randomness, chaoticity, periodicity, and fractalness [7].

Temporal series can show short- and/or long-term correlations. A parameter used to characterize these correlations is the Hurst exponent, which is much used in several science fields, such as astronomy [8], hydrology [9,10], physics [11], economy [12,13], and neuroscience [14]. Particularly in biological and medical areas, this exponent has been used as a health or disease marker [15]. For example, it is possible to distinguish between healthy and sick patients by analyzing the variation of the Hurst exponent from heart and brain data [16,17], which helps us to identify the patient's conditions and to predict heart attacks and epileptic seizures [18,19].

Despite the fact that temporal correlations are usually present in many data, the impact on predictability, as well as on information coded by a binary series, is not well

established. Considering the Hurst exponent $H = 0.5$ as a starting point since it represents the absence of temporal constraints, the increase or decrease of this value reflects whether the series is more persistent or antipersistent, respectively, which introduces changes in the probability of the patterns formed by 0's and 1's.

It should be stressed that mathematical approaches were previously developed to estimate entropy for time series in general, such as permutation entropy and others [7,20]. However, these methods do not take into account all pattern possibilities or the variability in the frequency of 0's and 1's, which is crucial in several fields, for example in information analysis of neuronal spike trains [21]. To fill this gap, we show the impact of the Hurst exponent, related to short- and long-range correlations, on the frequency of patterns embedded in a binary data series. We develop numerical and analytical solutions, proposing what we call the *Hurst entropy*. Our results link the informational entropy with a fractal-related parameter, which is highly important in several science fields [8–12,14,22–25]. We estimate that this approach can be very helpful in several areas in which evaluation of predictability is required or information as coded by binary data applies, as it might provide a more precise characterization of different sources of events as well as informational capability.

II. ENTROPY IN BINARY SERIES

We considered a binary series formed by sequences of 0s and 1's, which showed the probability of occurrence defined as p_0 and p_1 , respectively. The amount of information for such a discrete source can be calculated by Shannon's entropy (S), defined as

$$S = - \sum_{i=1}^N p_i \log_2(p_i), \quad (1)$$

*alexandre.kihara@ufabc.edu.br

where each i represents a code or a pattern and N is the quantity of them [26].

The amount of information also depends on the length of the patterns, whose occurrence in turn depends on the temporal correlations of the series. In order to evaluate the impact of temporal correlations for information and consequently the predictability of the temporal series, first we simulate a binary series based on a fractional stochastic process, as described below.

A. Binary series from fractional stochastic process

Fractional Brownian motion (fBm) is a self-similar Gaussian process $\{B^H(t), t > 0\}$, with zero mean, $\mathbb{E}[B^H(t)] = 0$, and covariance given by

$$\mathbb{E}[B^H(t_1)B^H(t_2)] = \frac{1}{2}(t_1^{2H} + t_2^{2H} - |t_1 - t_2|^{2H}) \quad (2)$$

for $t_1, t_2 \in \mathbb{R}$. The power exponent is the Hurst parameter, ranging from 0 to 1 ($0 < H < 1$). If $H = 0.5$, the motion has no memory corresponding to classical Brownian motion. If $H \neq 0.5$, the process exhibits memory, with two distinct behaviors. For $H < 0.5$, the process is antipersistent, and for $H > 0.5$, the process is persistent.

The fractional Gaussian noise (fGn) is the process $\{W^H(t), t > 0\}$ obtained from the increments of the fBm for discrete time as

$$W^H(t) = B^H(t + 1) - B^H(t). \quad (3)$$

The fGn is a stationary Gaussian process with zero mean and covariance given by

$$\begin{aligned} \rho(k) &= \mathbb{E}[W^H(t)W^H(t + k)] \\ &= \frac{1}{2}[(k + 1)^{2H} - 2k^{2H} + (k - 1)^{2H}] \end{aligned} \quad (4)$$

for $k > 0$. If $H = 1/2$, the process corresponds to white noise, since all correlations vanish. Here $\rho(k)$ shows an asymptotic behavior as $k \rightarrow \infty$ given by [27,28]

$$\frac{\rho(k)}{H(2H - 1)k^{2H-2}} \rightarrow 1. \quad (5)$$

If $1/2 < H < 1$, the correlations are not summable, $\sum_{-\infty}^{+\infty} \rho(k) = \infty$, a property of long-range dependence or long memory. And if $0 < H < 1/2$, the correlations are summable, $\sum_{-\infty}^{+\infty} \rho(k) = 0$, characterizing short-range dependence or short memory.

A binary series with short- and long-range dependence can be obtained from fGns with specific H . Using a desired threshold h , we can define a binary sequence,

$$\{s_t\}_{t=1,2,\dots,T}, \quad (6)$$

where T is the number of temporal intervals Δt , with two possible values, which are $s_t = 1$ if $W^H(t) > h$ or $s_t = 0$ if $W^H(t) \leq h$. For the sake of simplicity, and without loss of generality, we may consider $\Delta t = 1$.

The choice of h depends on p_1 , which is the probability of finding 1 in the respective series, and vice versa. Considering a normal distribution with mean zero and unit variance,

$$\int_h^{+\infty} \frac{1}{\sqrt{2\pi}} e^{-\frac{x^2}{2}} dx = p_1. \quad (7)$$

Therefore, solving the integral, we obtain

$$h = \sqrt{2}\text{erf}^{-1}(1 - 2p_1). \quad (8)$$

B. The impact of short- or long-range temporal correlations in the pattern occurrence of binary series

For the pattern length $L = 1$, the information entropy depends only on p_0 and p_1 and is given by Eq. (1). For lengths $L > 1$, the structure of the symbols in the series is important. For totally random sequences, the probability of a pattern of length L is just the multiplication of the individual probabilities of each symbol. See an example of random binary series, $H = 0.5$, in Fig. 1(a) for two values of p_1 , black series. Thus, the information entropy is given by

$$\begin{aligned} S(L) &= -p_0^L \log_2(p_0^L) - p_1^L \log_2(p_1^L) \\ &\quad - \sum_{i=1}^{L-1} C_L^i (p_1^i p_0^{L-i}) \log_2(p_1^i p_0^{L-i}), \end{aligned} \quad (9)$$

where

$$C_L^i = \frac{L!}{i!(L-i)!} \quad (10)$$

and $p_0 + p_1 = 1$.

For each value of L , we obtain an entropy curve, dependent on p_0 and p_1 . The maximum entropy, which happens when $p_0 = p_1$, grows linearly with N , the total number of patterns, which is $N = 2^L$, that is, $S(L)^{p_0=p_1=0.5} \propto N$. If we normalize by L , all curves collapse, with a maximum entropy rate of $S(L)/L$ equal to unity. The entropy rate is defined as $\lim_{L \rightarrow \infty} S(L)/L$ [21]; thus it reflects the amount of information in bits according to the length of the symbols as coded in the binary series [see Fig. 1(b), black curves]. This figure shows an example for pattern lengths $L = 1, 2, 3$, and 4, of the entropy rate plotted versus $1/L$.

When the series shows long or short-range dependence, even when probabilities p_1 and p_0 are maintained, the temporal correlations highly impact the pattern occurrence probabilities in the series. Figure 1(a) shows an example of the binary series with different values of p_1 and $H = 0.8$ (gray images). This can be observed comparing the series with $H = 0.5$ and $H = 0.8$ (black and gray images, respectively).

As the parameter H deviates from 0.5, the occurrence probabilities of the patterns of size L do not correspond to the multiplication of the individual probabilities p_0 or p_1 . For the cases when $H \neq 0.5$, the correlation term, Eq. (4), becomes relevant, changing the probabilities of the patterns. That way, considering for example $L = 2$ and $H > 0.5$, the probabilities of the patterns $\{11\}$ and $\{00\}$ are higher than expected when $H = 0.5$. On the other hand, when $H < 0.5$ these probabilities are smaller than expected when $H = 0.5$. These differences decrease the information entropy. Figure 1(b) shows an example comparing $H = 0.5$ and $H = 0.8$ (black and gray curves, respectively). As L increases, the entropy rate decreases for $H = 0.8$, while it exhibits a plateau for $H = 0.5$. The tendency of this decrease, or plateau, can be seen in the dashed lines drawn to the point $p_0 = p_1 = 0.5$.

The real entropy rate can be found by extrapolating the tendency line until it reaches the ordinate [21]. Therefore, the

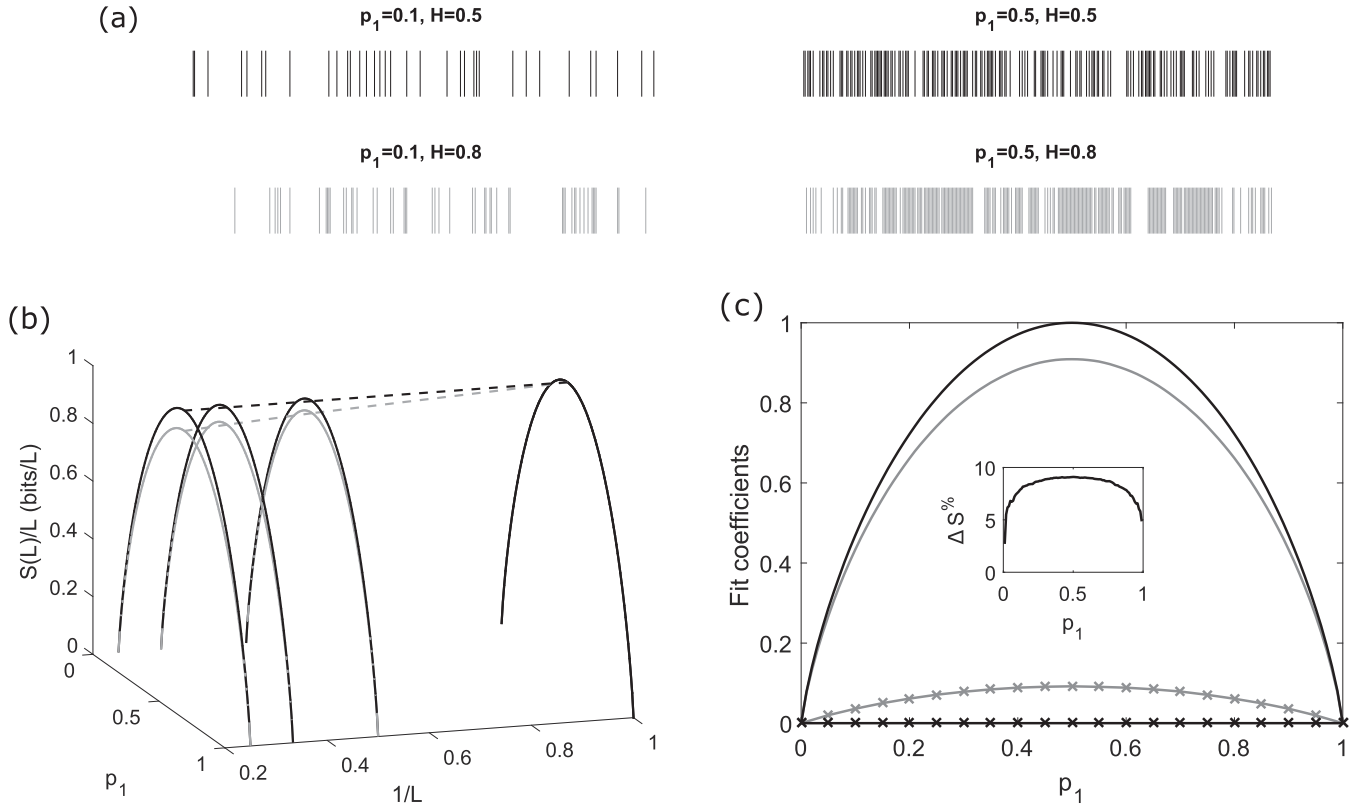


FIG. 1. (a) Examples of a binary series with $p_1 = 0.1$ and 0.5 and $H = 0.5$ (black lines) and 0.8 (gray lines). (b) Entropy rate $S(L)/L$ by $1/L$ and p_1 for two series with $H = 0.5$ (black lines) and $H = 0.8$ (gray lines). Dashed lines represent the tendency of the entropy rate for $p_1 = 0.5$. (c) Coefficients of the linear fit for the dashed lines. The continuous line represents the linear coefficients, and the x lines are the angular coefficients. The inset shows the relative drop in the entropy rate due to the temporal correlations, associated with the gain in predictability.

linear fit was calculated for the dashed curves for $p_1 = [0, 1]$. The coefficients of the fit are shown in Fig. 1(c), in which the linear coefficient is the real entropy rate (continuous line), and the angular coefficient is related to the slope (x line). The parameters R of the fits are higher than $R = 0.99$ for all cases.

The difference between the real entropy rates of $H = 0.8$ and $H = 0.5$ represents the impact of the temporal correlations in the information entropy rate. The relative drop in the entropy rate due to the temporal correlations is then defined as

$$\Delta S\% = 100 \left(1 - \frac{C^{H=0.8}}{C^{H=0.5}} \right), \quad (11)$$

where $C^{H=0.8}$ are the linear coefficients for the series with $H = 0.8$, and $C^{H=0.5}$ are the linear coefficients for the series with $H = 0.5$. The inset of Fig. 1(c) shows the drop comparing both cases.

With the decrease in the entropy, the predictability of the patterns in the temporal series is increased [29,30]. Indeed, entropy is considered the most fundamental measurement to quantify the degree of predictability of temporal series [29]. Therefore, the decrease of information entropy corresponds to gain in the predictability.

In this subsection we use the example displayed in Fig. 1 to show the impact of the temporal correlations on the information entropy rate and on the predictability of the series.

We employ the same procedure for a set of Hurst exponents, described in the next subsection.

C. Entropy from numerical simulations

We were able to calculate information entropy directly from our numerical simulations. From the binary series with $T = 10^6$, varying the values of H and p_1 , we calculated the entropy rate and the drop of the entropy rate. We varied the values as follows: $H = (0, 1)$ with intervals of 0.1 , and $p_1 = [0, 1]$ with intervals of 0.01 . The results are shown in Sec. II E.

D. Analytical solution

Besides the numerical approach, we proposed an analytical solution that includes the Hurst exponent in the calculation of the information entropy, referred to as *Hurst entropy*. Considering the linear approximation to obtain the entropy rate, we used the two first points, $L = 1$ and $L = 2$, to obtain an analytical approximation, as depicted below.

For patterns of length $L = 1$, the information entropy is

$$S_{L=1}^H = -p_1 \log_2(p_1) - (1 - p_1) \log_2(1 - p_1), \quad (12)$$

since $p_1 + p_0 = 1$.

If the length is $L = 2$, the possible patterns are $\{00\}$, $\{01\}$, $\{10\}$, and $\{11\}$, with probabilities p_{00} , p_{01} , p_{10} , and p_{11} . In

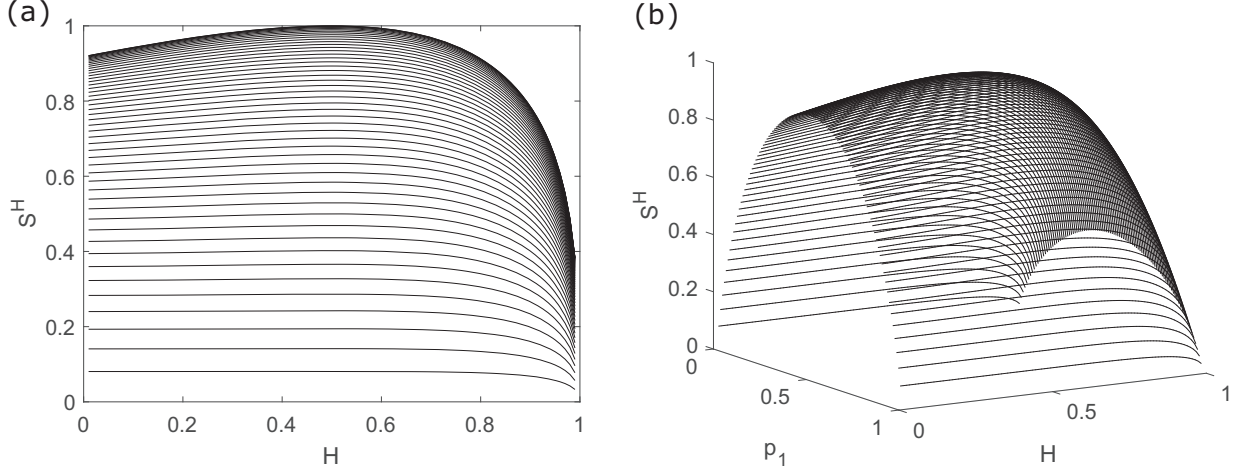


FIG. 2. The analytical solution of the entropy rate considering the Hurst exponent S^H . (a) View in two dimensions (2D) of S^H versus H . (b) View in 3D of S^H versus p_1 and H . Notice that each line represents distinct values of p_1 , and the lines show a symmetrical shape around $p_1 = 0.5$. These lines are the same as those represented in panel (a).

order to find out p_{11} , we considered the distribution

$$(Z_1 = W_t^H, Z_2 = W_{t+1}^H). \quad (13)$$

If (Z_1, Z_2) has a Gaussian distribution with mean zero and correlation coefficients

$$\rho_{ij} = \rho(Z_1, Z_2), \quad (14)$$

we can use Eq. (6) from Plackett [31] to find that

$$P(Z_1 > h, Z_2 > h) = p_1^2 + \frac{1}{2\pi} \int_0^{\rho_{12}} \frac{\exp[-h^2(1-\lambda)/(1-\lambda^2)]}{(1-\lambda^2)^{1/2}} d\lambda, \quad (15)$$

with

$$\rho_{12} = \rho(k=1) = 2^{2H-1} - 1. \quad (16)$$

The integral can be solved using the tableaus of bivariate normal distributions [32] or can be solved numerically. The integral term on the right side of Eq. (15) is responsible for the increase, or decrease, of the pattern probability p_{11} dependent on H .

For the case where $p_1 = p_0 = \frac{1}{2}$, we have the particular case where $h = 0$ [33], which is

$$P(Z_1 > 0, Z_2 > 0) = \frac{1}{4} + \frac{1}{2\pi} \arcsin(\rho_{12}). \quad (17)$$

If $H = 0.5$, $\rho_{12} = 0$, and

$$P(Z_1 > h, Z_2 > h) = p_1^2, \quad (18)$$

we can write $p_1 = p_{10} + p_{11}$, so $p_{10} = p_1 - p_{11}$. We also have, as $p_{10} = p_{01}$, that $p_{11} + 2p_{10} + p_{00} = 1$, so $p_{00} = 1 - p_{11} - 2p_{10}$. Summarizing

$$p_{11} = p_1^2 + \frac{1}{2\pi} \int_0^{\rho_{12}} \frac{\exp[-h^2(1-\lambda)/(1-\lambda^2)]}{(1-\lambda^2)^{1/2}} d\lambda, \quad (19)$$

$$p_{10} = p_{01} = p_1 - p_{11},$$

$$p_{00} = 1 - p_{11} - 2p_{10} = 1 - 2p_1 + p_{11}.$$

The entropy can be calculated as

$$S_{L=2}^H = -p_{11} \log_2(p_{11}) - p_{00} \log_2(p_{00}) - 2p_{10} \log_2(p_{10}). \quad (20)$$

In order to find the Hurst entropy rate S^H , we calculated

$$S^H = S_{L=2}^H - S_{L=1}^H. \quad (21)$$

Figure 2 shows the analytical approximation for the Hurst entropy rate S^H varying $p_1 = [0, 1]$ and $H = (0, 1)$, with intervals of 0.01. The maximum unpredictability occurs with $H = 0.5$ and $p_1 = 0.5$, showing a nonsymmetrical decaying as H moves away from 0.5. As p_1 moves away from 0.5, the impact of H on S^H decreases. For low p_1 s, S^H almost does not change for $H < 0.5$, showing little decay for $H > 0.5$.

The relative drop of the entropy rate $\Delta S^{\%}$ dependent on H can be calculated as

$$\Delta S^{\%} = 100 \left(1 - \frac{S^H}{S^{H=0.5}} \right) \quad (22)$$

and is shown in Fig. 3. As H moves away from 0.5, the larger is the gain in the predictability, especially when $H > 0.5$.

E. Comparison between analytical and numerical solutions

The analytical solution can be compared with our previous simulations. Figure 4 shows that the simulation data points (black dots) overlies the analytical solution (gray lines). The rms error between simulations and analytical solutions was calculated as

$$E = \sqrt{\frac{\sum_{j=1}^N (S_{anal}^{H^j} - S_{simul}^{H^j})^2}{N}}. \quad (23)$$

Considering all simulations, $N = 909$, the value was $E = 0.0089$. Besides only two lengths L were used, $L = 1$ and $L = 2$, and the error is very small, revealing that this approach is useful.

The rms error for the relative drop was also calculated; the result was the value 1.15.

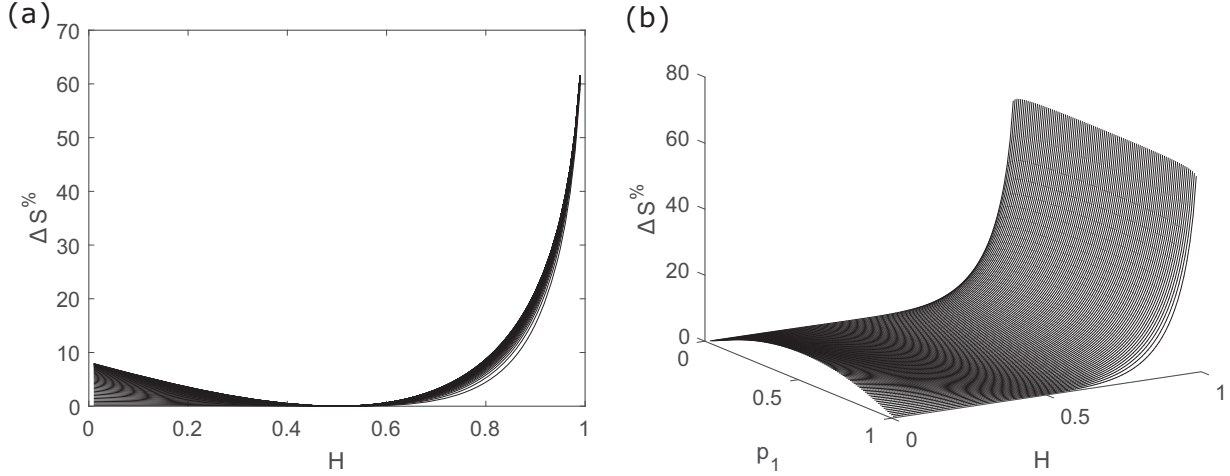


FIG. 3. The analytical solution for the relative drop of the entropy rate considering the Hurst exponent $\Delta S\%$. (a) View in 2D of $\Delta S\%$ versus H . (b) View in 3D of $\Delta S\%$ versus p_1 and H .

III. REAL DATA

The previous examples were restricted to a series with single values of the Hurst exponent H and p_1 . However, real data can show a more complex behavior, with H and p_1 being variable with time. In the case in which it is possible to identify n subsamples i of temporal length T^i in the series, in which each subsample owns a value of exponent H^i and p_1^i , we can estimate the Hurst entropy considering this spectrum of H 's and p_1 's. In order to estimate the entropy and the entropy rate of such a source, we first determine the new pattern probabilities by lengths L , indicated by the symbol $*$. So, for length $L = 1$, the estimated p_1^* is

$$p_1^* = \frac{\sum_{i=1}^n p_1^i T^i}{\sum_{i=1}^n T^i}, \quad (24)$$

and $p_0^* = 1 - p_1^*$.

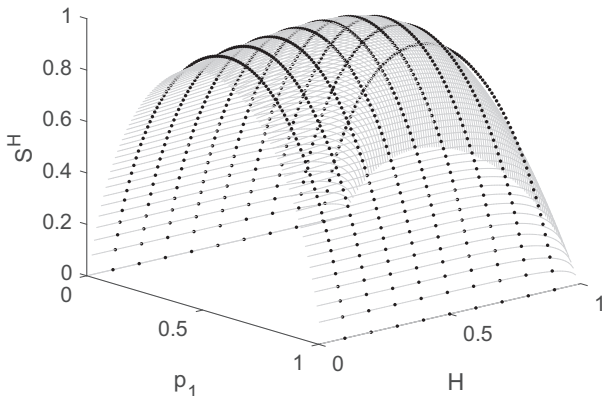


FIG. 4. Graphical representation of the Hurst entropy rate S^H obtained from simulations (black dots) for $H = (0, 1)$ with intervals of 0.1 and $p_1 = [0, 1]$ with intervals of 0.01. The simulation results overlies the analytical solution (gray lines).

For length $L = 2$, the estimated probability p_{11}^* is

$$p_{11}^* = \frac{\sum_{i=1}^n p_{11}^i (p_1^i, H^i) T^i}{\sum_{i=1}^n T^i}, \quad (25)$$

where $p_{11}^i(p_1^i, H^i)$ is the probability of the pattern $\{11\}$ dependent on p_1^i and H^i , and is given by Eq. (15). The other probabilities are calculated as before through Eqs. (19). Since all probabilities were found, we can estimate the information entropies, $S_{L=1}^{*H}$ and $S_{L=2}^{*H}$, and the Hurst entropy rate S^{*H} .

IV. CONCLUSION

Herein, we proposed a method based on a fractal-related process to quantify the increase of the predictability in binary time series with short or long-range temporal correlations. As seen, the autocorrelation reflects an increase, or decrease, in the occurrence of the patterns formed by 0's and 1's, as described in the analytical solution in Sec. II D. Although our approach takes into consideration only two lengths of patterns, the rms error was very small, revealing its accuracy.

We considered $\Delta t = 1$, and it is possible to associate our solution with real temporal data by multiplying the entropy rate by the inverse of the temporal resolution $1/\Delta t$. Additionally, our parameter p_1 is related to the rate r of the occurrence of the symbol 1 and can be calculated as $r = \frac{p_1}{\Delta t}$.

We estimate that this approach can be very helpful for several areas in which binary data apply, including neuroscience and econophysics, as it might provide a more precise characterization of different sources of information.

ACKNOWLEDGMENTS

We acknowledge H. Silva, F. Borges, E. Kinjo, and G. Higa for scientific discussions. This research was supported by Grant No. 2015/50122-0 from the São Paulo Research Foundation (FAPESP), the DFG (Grant No. IRTG1740/2), the FAPESP (Grant No. 2017/26439-0), and the CNPq (Grants No. 312047/2017-7, No. 431000/2016-6, and No. 154130/2018-4).

- [1] J. Aljadeff, B. J. Lansdell, A. L. Fairhall, and D. Kleinfeld, *Neuron* **91**, 221 (2016).
- [2] A. Lipowski, D. Lipowska, and A. L. Ferreira, *Phys. Rev. E* **96**, 032145 (2017).
- [3] D. Escaff, R. Toral, C. V. den Broeck, and K. Lindenberg, *Chaos* **28**, 075507 (2018).
- [4] L. S. Liebovitch and J. M. Sullivan, *Biophys. J.* **52**, 979 (1987).
- [5] S. Aki and K. Hirano, *Ann. Inst. Statist. Math.* **46**, 193 (1994).
- [6] J.-P. Bouchaud and R. Cont, *Eur. Phys. J. B* **6**, 543 (1998).
- [7] H. V. Ribeiro, M. Jauregui, L. Zunino, and E. K. Lenzi, *Phys. Rev. E* **95**, 062106 (2017).
- [8] C. Federrath, R. S. Klessen, and W. Schmidt, *Astrophys. J.* **692**, 364 (2009).
- [9] B. B. Mandelbrot and J. Wallis, *Water Resour. Res.* **4**, 909 (1968).
- [10] T. Iliopoulou, S. M. Papalexioiu, Y. Markonis, and D. Koutsoyiannis, *J. Hydrol. (Amsterdam, Neth.)* **556**, 891 (2018).
- [11] M. Gilmore, *Phys. Plasmas* **9**, 1312 (2002).
- [12] A. Carbone, G. Castelli, and H. E. Stanley, *Phys. A (Amsterdam, Neth.)* **344**, 267 (2004).
- [13] D. Grech and Z. Mazur, *Phys. A (Amsterdam, Neth.)* **336**, 133 (2004).
- [14] J. Dong, B. Jing, X. Ma, H. Liu, X. Mo, and H. Li, *Front. Neurosci.* **12**, 34 (2018).
- [15] H. Kantz, J. Kurths, and G. Mayer-Kress, *Nonlinear Analysis of Physiological Data* (Springer, Berlin, 1996).
- [16] S. Havlin, L. A. N. Amaral, Y. Ashkenazy, A. L. Goldberger, P. C. Ivanov, C.-K. Peng, and H. E. Stanley, *Phys. A (Amsterdam, Neth.)* **274**, 99 (1999).
- [17] M. O. Sokunbi, V. B. Gradin, G. D. Waiter, G. G. Cameron, T. S. Ahearn, A. D. Murray, D. J. Steele, and R. T. Staff, *PLoS One* **9**, e95146 (2014).
- [18] T. Kuusela, *Phys. Rev. E* **69**, 031916 (2004).
- [19] H. Namazi, V. V. Kulish, J. Hussaini, J. Hussaini, A. Delaviz, F. Delaviz, S. Habibi, and S. Ramezani, *Ontotarget* **7**, 342 (2016).
- [20] C. Bandt and B. Pompe, *Phys. Rev. Lett.* **88**, 174102 (2002).
- [21] S. P. Strong, R. Koberle, R. R. de Ruytervan Steveninck, and W. Bialek, *Phys. Rev. Lett.* **80**, 197 (1998).
- [22] B. B. Mandelbrot and J. W. V. Ness, *SIAM Rev.* **10**, 422 (1968).
- [23] D. Brogioli and A. Vailati, *Phys. Rev. E* **96**, 012136 (2017).
- [24] F. Patzelt and J.-P. Bouchaud, *Phys. Rev. E* **97**, 012304 (2018).
- [25] F. von Wegner, H. Laufs, and E. Tagliazucchi, *Phys. Rev. E* **97**, 022415 (2018).
- [26] C. E. Shannon and E. Weaver, *The Mathematical Theory of Communication* (Illinois Press, Urbana, IL, 1949).
- [27] J. Beran, *Statistics for Long-Memory Process*, Monographs on Statistics and Applied Probability Vol. 61 (Chapman & Hall, London, 1994).
- [28] G. Samorodnitsky, *Found. Trends Stochastic Syst.* **1**, 163 (2006).
- [29] C. Song, Z. Qu, N. Blumm, and A.-L. Barabási, *Science* **327**, 1018 (2010).
- [30] S.-M. Qin, H. Verkasalo, M. Mohtaschemi, T. Hartonen, and M. Alava, *PLoS ONE* **7**, e51353 (2012).
- [31] R. L. Plackett, *Biometrika* **41**, 351 (1954).
- [32] U. States, *National Bureau of Standards: Tables of the Bivariate Normal Distribution and Related Functions* (U.S. Government Printing Office, Washington, 1959).
- [33] R. H. Bacon, *Ann. Math. Statist.* **34**, 191 (1963).